Pergamon

Tetrahedron 55 (1999) 3605–3614

TETRAHEDRON

Asymmetric Addition of Dialkylzincs to Benzaldehyde Derivatives Catalyzed by Chiral β-Amino Alcohols. Evidence for the Monomeric Alkylzinc Aminoalkoxide as Catalyst†

Masato Kitamura, Hiromasa Oka, and Ryoji Noyori*

Department of Chemistry and Molecular Chirality Research Unit, Nagoya University
Chikusa, Nagoya 464-8602, Japan

Received 16 March 1998; revised 28 April 1998; accepted 29 April 1998

Abstract: 3-*exo*-(Dimethylamino)isoborneol efficiently promotes the asymmetric addition of dialkylzincs to aldehydes. In order to characterize the catalytic organozinc species, relative reactivities of various substituted benzaldehydes and organozincs have been examined under enantiopure and racemic conditions. The relative rates are not affected by the enantiomeric purity of the amino alcohol. The Hammett plots of methylation of *p*-substituted benzaldehydes gave a ρ value of +1.2. Methylation of *o*-methylbenzaldehyde is slower than that of benzaldehyde by a factor of 2.3. Relative reactivities of $(CH_3)_2Zn$, $(C_2H_5)_2Zn$, and $(n\text{-}C_4H_9)_2Zn$ with benzaldehyde were 1:21:8. The results strongly support the mechanism involving a monomeric alkylzinc aminoalkoxide as catalyst.

1. BACKGROUND

In the presence of a small amount of (2*S*)- or (2*R*)-3-*exo*-(dimethylamino)isoborneol [(2*S*)- or (2*R*)-DAIB], dialkylzincs react with aldehydes in toluene to give after aqueous workup the corresponding secondary alcohols in high ee.[1] The most intriguing phenomenon in this asymmetric catalysis is the nonlinear relationship between the enantiomeric purity of the chiral source, DAIB, and that of the alcoholic products.[2–6] For example, methylation of benzaldehyde with (2*S*)-DAIB in 20% ee produces (*S*)-1-phenylethanol in 88% ee,[7] a value close to the 95% ee obtained with enantiomerically pure (2*S*)-DAIB. In addition, the reaction rate is significantly influenced by the enantiomeric purity of DAIB; the methylation catalyzed by enanatiomerically pure DAIB is significantly faster than the reaction using the racemic amino alcohol.[7] Our earlier structural study elucidated that (2*S*)- or (2*R*)-DAIB reacts with dimethylzinc by elimination of methane to produce the tricoordinate methylzinc aminoalkoxide, ***S*** or ***R***, which forms dimeric structures in a reversible manner.[8–10] Homochiral dimerization leads to the chiral dimers, ***S–S*** and ***R–R***, while the heterochiral interaction forms the meso dinuclear complex, ***S–R***. The asymmetric catalysis has been thought to involve the monomer ***S*** or ***R*** acting as a bifunctional catalyst.[11–13] The Zn atom provides a Lewis-acidic site which accepts an aldehyde substrate, while the oxygen is a basic center that interacts with a dialkylzinc. Thus alkylation would proceed

---

†Dedicated to the memory of Professor Sir Derek Barton who made an outstanding contribution to the development of Organic Chemistry.

PII: S0040-4020(98)01167-3

via a ternary complex of ***S*** (or ***R***), aldehyde, and dialkylzinc.[11–13] The chirality amplification effect has been interpreted to be a result of competition of the enantiomorphic *S* and *R* catalytic cycles as shown schematically in Figure 1, where ***S*** leads to the *S*-enriched product and ***R*** gives the *R* isomer preferentially. The far higher stability of ***S–R*** compared to ***S–S*** or ***R–R*** would result in a marked amplification of the chirality as well as making the rate dependent on the enantiomeric purity of DAIB.[14] However, there is an alternative possibility. As illustrated in Figure 2, the nonlinear phenomena may originate from the competition of the diastereomorphic catalytic cycles, *S–S* or *R–R* cycle vs *S–R* cycle.[15,16] The dimeric Zn complexes might directly interact with benzaldehyde and then dialkylzinc, or vice versa, to enter into the catalytic cycle.

The differentiation of the monomer and dimer mechanisms has remained difficult despite extensive structural studies on the dinuclear Zn complexes using cryoscopic and vapor pressure osmometric molecular weight determination,[10] calorimetric study,[10] dynamic NMR, X-ray crystallographic analysis,[8,9,14] and MO calculations.[11] The dissociation constants of ***S–S*** and ***S–R*** differ significantly, $K_{\text{homo}} = (3.0 \pm 1.0) \times 10^{-2}$ M vs $K_{\text{hetero}} = 1 \times 10^{-5}$ M (toluene, 40 °C). Thus, in a 10 mM toluene solution, ca. 60% of ***S–S*** exists as monomer ***S***, while only 3% of ***S–R*** dissociates to the racemic monomers, ***S*** + ***R***, although the dissociation of the dimers is facilitated by the addition of dimethylzinc or benzaldehyde which shift the equilibrium. As shown

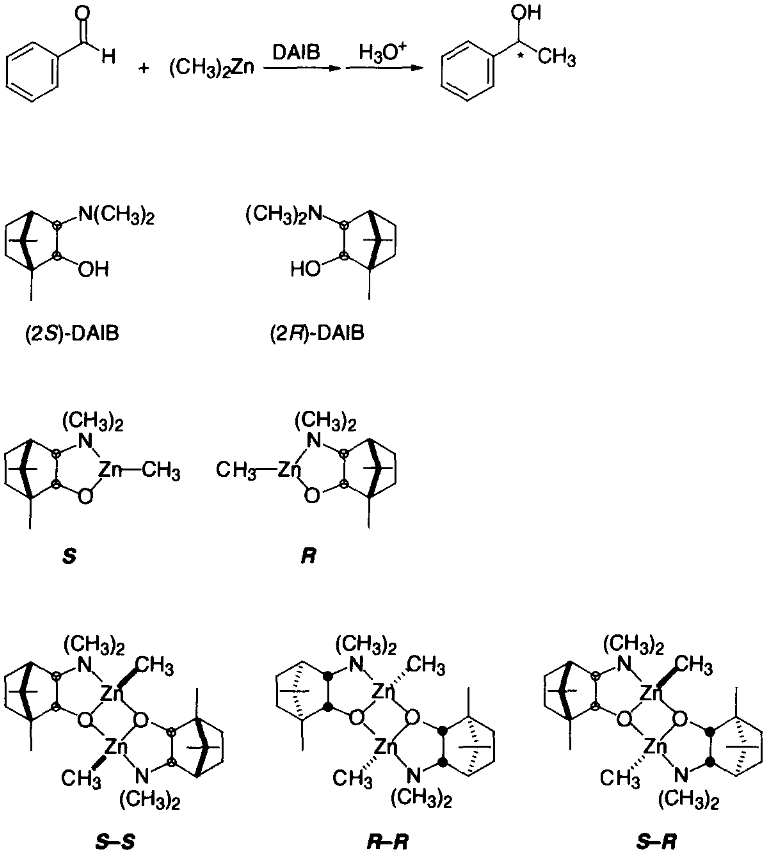

by NMR analysis, the dimeric structure of ***S–S*** is readily ruptured by the addition of dimethylzinc or benzaldehyde, while the spectrum of ***S–R*** does not change with the addition of the reagent and/or substrate. Saturation-transfer experiments revealed the rate constant of dissociation of ***S–R*** to be 1.7 x 10^{-1} s^{-1}. This value is two orders of magnitude higher than the constant of the rate-limiting alkyl migration from the *S*/dimethyzinc/aldehyde mixed-ligand complex in the (2*S*)-DAIB-promoted methylation, 4.2 x 10^{-3} s^{-1}. The kinetic profiles of the reactions with (2*S*)- and (±)-DAIB are different. In the reaction using DAIB in 100% ee,

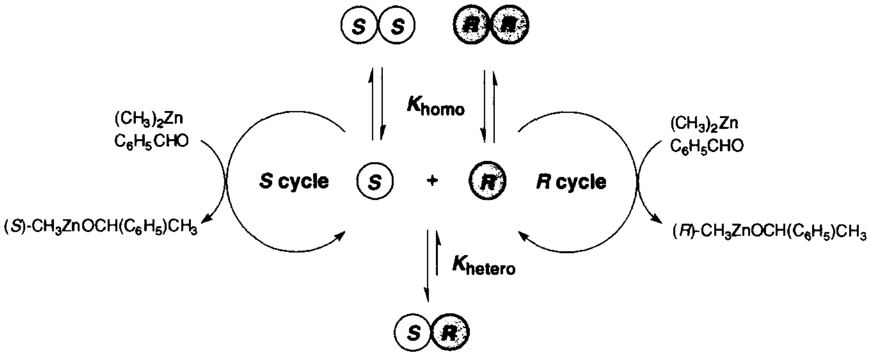

Figure 1. Monomer mechanism.

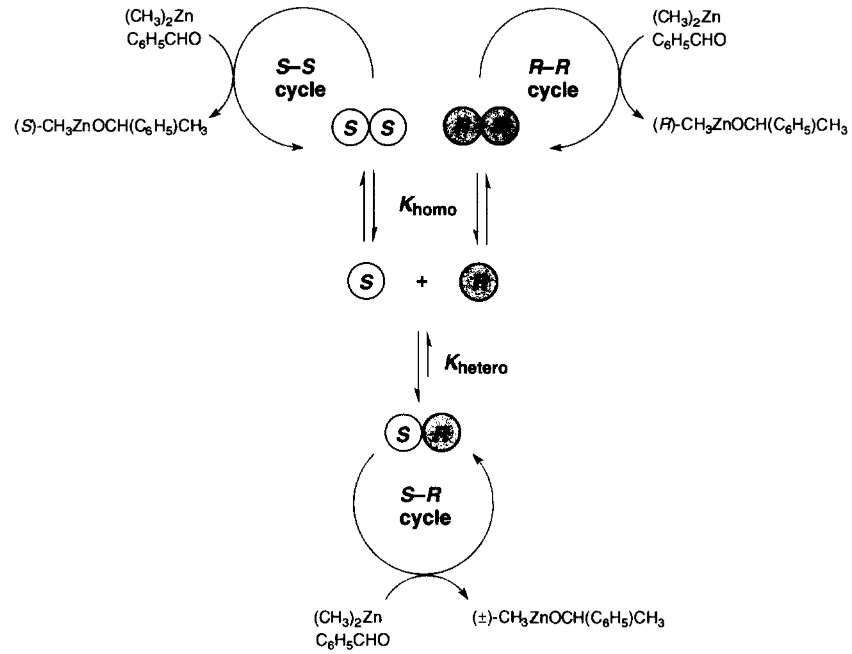

Figure 2. Dimer mechanism.

the rate is readily maximized by increasing the concentrations of dimethylzinc and benzaldehyde.[8] On the other hand, the reaction with racemic DAIB does not reach saturation kinetics even with high concentrations of the reagent and substrate. Thus, stable ***S–R*** does liberate monomeric *S* and ***R*** under standard catalytic conditions but the contribution of the dinuclear complex prior to dissociation is still a possibility.

Since the earlier investigations did not clearly distinguish between the two mechanisms, we intended to solve this problem by a purely chemical means.

2. RESULTS AND DISCUSSION

Enantiomeric *S* and ***R*** have the same atomic constituent, connectivity, and spatial arrangement. If the monomer is the true catalyst as shown in Figure 1, the relative reactivities of different substituted benzaldehydes and different dialkylzincs should be independent of whether the DAIB auxiliary is enantiomerically pure or racemic. On the other hand, when diastereomeric ***S–S*** (or ***R–R***) and ***S–R*** directly participate in the step associated with the turnover rate of catalysis (Figure 2), relative reactivities of the different aldehydes or diorganozincs would be strongly affected by the enantiomeric purity of DAIB. A similar trend is expected when the two mechanisms coexist in the catalytic reaction or if there is a mechanistic change between the reactions promoted by (2*S*)- and (±)-DAIB. We here present experimental support for the monomer mechanism of Figure 1.

First, we examined the relative reactivities of benzaldehyde (**1a**) and its derivatives **1b–e** possessing different ring substituents. The reaction was conducted using a 1:1 mixture of benzaldehyde and a *para*-substituted benzaldehyde (each 210 mM), dimethylzinc (420 mM), and (2*S*)-DAIB (8 mM) in toluene at 40 °C. The methylation was interrupted at <20% conversion and aliquots were analyzed by GC and/or HPLC. As illustrated in Table 1, the competitive experiments revealed that the presence of an electron-withdrawing group at the para position increases the reactivity of aldehydes. The *p*-CF_3 derivative **1b** is 6 times more reactive than parent benzaldehyde **1a**, while the reactivity of the *p*-OCH_3 derivative **1e** is about half of **1a**. The Hammett plot using the standard σ_p constants for the substituent parameters exhibits a linear free-energy relationship with a ρ value of +1.2 (Figure 3a). The presence of electron-withdrawing substituents at the para position tends to increase the enantioselectivity, ranging from 86% ee (*p*-OCH_3) to 96% ee (*p*-CF_3) (Table 1). When racemic DAIB was used as an auxiliary, under otherwise identical conditions, the reaction became ca. 6 times slower compared to the reaction using pure (2*S*)-DAIB. However the relative reactivities of **1a–e** remained unchanged (Table 1), the ρ value being +1.2 as shown in Figure 3b.

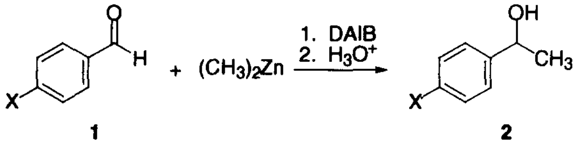

a: X = H d: X = CH_3
b: X = CF_3 e: X = OCH_3
c: X = Cl

Table 1. Reactivity and Stereoselectivity in the DAIB-Promoted Methylation of Benzaldehydes

X in *p*-XC_6H_4CHO	% ee of (2*S*)-DAIB	v_{OX}/v_{OH}	% ee of product
CF_3	100	6.0	96
	0	5.7	—
Cl	100	2.4	94
	0	2.5	—
H	100	1.0	95
	0	1.0	—
CH_3	100	0.90	94
	0	0.89	—
OCH_3	100	0.55	88
	0	0.57	—

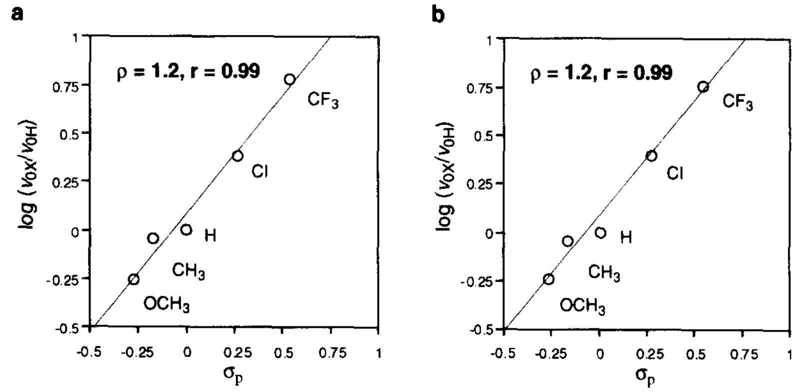

Figure 3. Hammett plots for the DAIB-promoted methylation of benzaldehydes **1a–e**. **a**: the initial rate ratio/σ_p relation with (2*S*)-DAIB in 100% ee. **b**: the initial rate ratio/σ_p relation with (±)-DAIB.

The extent of steric effect is also identical in reactions using (2*S*)-DAIB and (±)-DAIB. When dimethylzinc (420 mM) was subjected to a reaction with a 1:1 mixture of benzaldehyde (**1a**) and the *ortho*-methylated derivative **1f** in the presence of DAIB (8 mM) in toluene at 40 °C, **2a** and **2f** were obtained in a ratio of 1:0.43 regardless of the enantiomeric purity of DAIB, either 100% ee or 0% ee. These investigations of the electronic and steric factors indicate the operation of a single, common mechanism involving the monomeric catalyst ***S*** or ***R***.

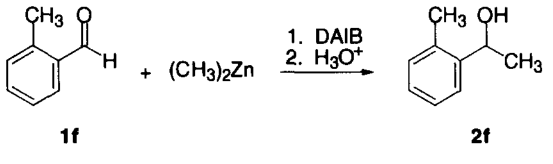

The relative reactivities of dimethylzinc, diethylzinc, and di-*n*-butylzinc were then compared under enantiopure and racemic conditions. An 8 mM DAIB solution in toluene was first treated with $R^1{}_2Zn$ (210 mM) and subsequently a different diorganozinc $R^2{}_2Zn$ (210 mM) and benzaldehyde (**1a**) (420 mM) were added. The mixture was kept at 40 °C, hydrolyzed, and analyzed by GC. Table 2 summarizes the ratio of the R^1- and R^2-products of these experiments. Regardless of the enantiomeric purity of DAIB, 100% ee or 0% ee, a similar reactivity ratio, CH_3:C_2H_5:*n*-C_4H_9 = 1:21:8, was observed.[8] The order of addition of the two organozincs did not affect the product ratio.

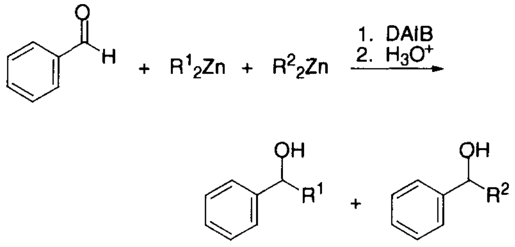

Table 2. Relative Reactivity of $(CH_3)_2Zn$, $(C_2H_5)_2Zn$, and $(n\text{-}C_4H_9)_2Zn$ toward Benzaldehyde

dialkylzincs		% ee of (2*S*)-DAIB	ratio		relative reactivity R^1:R^2
$R^1{}_2Zn$	$R^2{}_2Zn$		C_6H_5-$CH(OH)R^1$	C_6H_5-$CH(OH)R^2$	
CH_3	C_2H_5	100	5.0	95.0	1:19
		0	4.3	95.7	1:22
C_2H_5	CH_3	100	95.5	4.5	21:1
		0	95.5	4.5	21:1
CH_3	*n*-C_4H_9	100	11.6	88.4	1:8
		0	11.5	88.5	1:8
n-C_4H_9	CH_3	100	88.4	11.6	8:1
		0	87.0	13.0	7:1

These competitive experiments provide strong support for a common mechanism involving monomeric catalyst *S* or ***R***. The coexistence of the monomer and dimer mechanisms or a change in the turnover-limiting step is also unlikely. Under standard conditions, not only unstable *S–S* and ***R–R*** but also stable ***S–R*** dissociates into the monomers prior to reacting with dialkylzincs and aldehydes.[17]

3. EXPERIMENTAL

All experiments were performed under an argon atmosphere using standard Schlenk techniques. The preparation and purification of chemicals and the procedures for alkylation and NMR analysis are essentially the same as those reported.[8,9]

Chemicals

Chemicals were all stored in Schlenk tubes equipped with a Young's tap. Toluene and toluene-d_8 were distilled over a Na–K alloy. Commercial dimethylzinc (Toyo Stauffer Chemical Co., Lot No. DMZ-812) was distilled at 25 °C and at 0.01 mmHg. The purified dimethylzinc (9.76 g, 0.102 mol) was diluted with toluene to a total volume of 30 mL under an argon stream. The resulting 3.41 M toluene solution was kept at –30 °C in the dark. The solutions were used within 3 weeks. Freshly distilled dimethylzinc was used in the reaction with benzaldehyde and gave the product in 95% ee. Commercial diethylzinc (Toyo Stauffer Chemical Co., Lot No. DEZ-948) and di-*n*-butylzinc prepared according to the reported method[18] were distilled at 0.01 mmHg and at 25 and 40 °C, respectively. The stock toluene solutions of diethylzinc (3.47 M) and di-*n*-butylzinc (2.81 M) were prepared and stored in a similar way to that for dimethylzinc. Optically pure (2*S*)-DAIB and racemic DAIB were synthesized by the reported method.[8] Benzaldehyde (**1a**), purchased from Nacalai Tesque, was distilled over molecular sieves 4A at 70.5–71.5 °C at 20 mmHg. *p*-Trifluoromethylbenzaldehyde (**1b**) and *p*-methylbenzaldehyde (**1d**) were purchased from Tokyo Chemicals while *p*-chlorobenzaldehyde (**1c**) and *p*-methoxybenzaldehyde (**1e**) were from Nacalai Tesque. *o*-Methylbenzaldehyde (**1f**) was purchased from Kanto Chemicals. The aldehydes **1b**, **1d**, **1e**, and **1f** were distilled, before use, over molecular sieves 4A. Compound **1c** was recrystallized from a 3:1 mixture of ethanol and water.

Analytical methods

The extent of conversion was determined by GC analysis using a Shimadzu GC-17A gas chromatograph: The conditions [capillary column, GL Scientific DB-WAX 0.25 mm x 15 m; column temperature, 90 °C; rate of temperature increase, 5 °C min^{-1}; carrier gas, He; flow rate, 171 mL min^{-1}; split ratio, 39:1] afforded good separation of the following compounds with t_R values in parentheses: **1a** (2.6 min), **1b** (2.0 min), **1c** (5.8 min), **1d** (4.1 min), **1e** (10.2 min), **1f** (3.7 min), **2a** (6.7 min), **2b** (7.6 min), **2c** (12.4 min), **2d** (8.1 min), **2e** (13.7 min), **2f** (8.8 min), 1-phenyl-1-propanol (7.6 min), 1-phenyl-1-pentanol (11.0 min), benzyl alcohol (7.5 min).[1,19,20]

The product ee's were determined by HPLC or GC analysis. Under the conditions [apparatus, Shimadzu LC-6A model; column, Daicel CHIRALCEL OB-H; eluent, 100:2 hexane–2-propanol; flow rate, 1.0mL min^{-1}; detection, 254-nm light], the following enantiomers were separated with t_R values indicated in parentheses: **2a** (13.5 min (*S*), 22.4 min (*R*)), **2c** (12.1 min (*S*), 13.8 min (*R*)), **2d** (12.4 min (*S*), 15.3 min (*R*)). Enantiomers of **2e** were separated (30.0 min (*S*), 40.6 min (*R*)) using Daicel CHIRALPAK AS under the same conditions as with CHIRALCEL OB-H. The enantiomer ratio of **2b** was determined by GC using a Shimadzu GC-17A (capillary column, Tokyo Kasei G-TA 0.25 mm x 30 m; column temperature, 100 °C; carrier gas, He; flow rate, 171 mL min^{-1}; split ratio, 79:1; t_R, 11.0 min (*R*) and 11.7 min (*S*)).

The absolute configurations of **2b–e** obtained by use of (*S*)-DAIB were determined by comparison of the sign of optical rotations with those reported.[19] **2b**: $[\alpha]^{25}_D$ –22.8° (c 1.14, CH_3OH) [lit. $[\alpha]^{21}_D$ +29.8° (c 1.088, CH_3OH) for (*R*)-**2b**]. **2c**: $[\alpha]^{25}_D$ –31.4° (c 1.06, CH_3OH) [lit. $[\alpha]^{21}_D$ +39.8° (c 1.064, CH_3OH) for (*R*)-**2c**)]. **2d**: $[\alpha]^{25}_D$ –37.3° (c 1.02, CH_3OH) [lit. $[\alpha]^{21}_D$ +43.8° (c 0.914, CH_3OH) for (*R*)-**2d**]. **2e**: $[\alpha]^{25}_D$ –23.1° (c 0.93, CH_3OH) [lit. $[\alpha]^{21}_D$ +41.0° (c 1.069, CH_3OH) for (*R*)-**2e**]. For **2a**, see ref 8.

Kinetic experiments

The initial rates of alkylation of **1a** and its derivatives **1b–f** were compared in a competitive experiment using [DAIB] = 8 mM, [DMZ] = 420 mM, and [**1a**] = [**1b–f**] = 210 mM. Listed below are the data (reaction time (min), % conversion of **1a**, and % conversion of **1b–f**), initial rate of **1a**, initial rate of **1b–f**, and rate ratio for each compound. **1b** with (2*S*)-DAIB: data (20, 4.3, 26.5), 0.45 mM min^{-1}, 2.7 mM min^{-1}; 6.0. **1b** with (±)-DAIB: data (120, 5.1, 28.8), 0.089 mM min^{-1}, 0.50 mM min^{-1}, 5.7. **1c** with (2*S*)-DAIB: data (30, 5.1, 12.4), 0.36 mM min^{-1}, 0.87 mM min^{-1}, 2.4. **1c** with (±)-DAIB: data (120, 4.7, 11.6), 0.081 mM min^{-1}, 0.20 mM min^{-1}, 2.5. **1d** with (2*S*)-DAIB: data (40, 10.3, 9.3), 0.54 mM min^{-1}, 0.49 mM min^{-1}, 0.90. **1d** with (±)-DAIB: data (240, 11.6, 10.2), 0.10 mM min^{-1}, 0.089 mM min^{-1}, 0.89. **1e** with (2*S*)-DAIB: data (50, 14.0, 7.7), 0.59 mM min^{-1}, 0.33 mM min^{-1}, 0.55. **1e** with (±)-DAIB: data (300, 14.8, 8.2), 0.10 mM min^{-1}, 0.057 mM min^{-1}, 0.57. **1f** with (2*S*)-DAIB: data [(15, 4.3, 1.7), (30, 7.9, 3.4), (45, 11.6, 4.9), (60, 14.8, 6.5), (75, 18.3, 7.9), (90, 23.1, 10.2), (105, 26.7, 11.3)], 0.53 mM min^{-1}, 0.23 mM min^{-1}, 0.43. **1f** with (±)-DAIB: data [(100, 4.4, 1.8), (180, 7.1, 3.3), (270, 11.4, 4.8), (360, 13.9, 6.3), (450, 17.6, 8.0), (540, 23.7, 10.1)], 0.088 mM min^{-1}, 0.038 mM min^{-1}, 0.43. With optically pure DAIB, the ee of **2a**, **2b**, **2c**, **2d**, and **2e** ranged from 93.6–94.5%, 95.0–96.3%, 93.4–93.8%, 93.9–94.1%, and 83.3–88.1%, respectively.

The initial rate ratios of the reaction of R^1_2Zn and R^2_2Zn were determined with [DAIB] = 8 mM, [R^1_2Zn] = [R^2_2Zn] = 210 mM, and [**1a**] = 420 mM. Reactions were carried out by mixing in the order of DAIB, R^1_2Zn, R^2_2Zn, and **1a**. Listed below are the data (reaction time (min), % yield of the R^1 adduct,[1] and % yield of R^2 adduct[1]), initial rate of addition of R^1, initial rate of addition of R^2, and rate ratio for each reaction. $R^1 = CH_3$, $R^2 = C_2H_5$, (2*S*)-DAIB: data (20, 3.1, 59.3), 0.33 mM min^{-1}, 6.2 mM min^{-1}, 1:19. $R^1 = CH_3$, $R^2 = C_2H_5$, (±)-DAIB: data (60, 2.0, 44.8), 0.070 mM min^{-1}, 1.6 mM min^{-1}, 1:22. $R^1 = C_2H_5$, $R^2 = CH_3$, (2*S*)-DAIB: data (20, 67.5, 3.2), 7.1 mM min^{-1}, 0.34 mM min^{-1}, 21:1. $R^1 = C_2H_5$, $R^2 = CH_3$, (±)-DAIB: data (60, 44.7, 2.1), 1.6 mM min^{-1}, 0.074 mM min^{-1}, 21:1. $R^1 = CH_3$, $R^2 = n\text{-}C_4H_9$, (2*S*)-DAIB: data (20, 2.4, 18.2), 0.25 mM min^{-1}, 1.9 mM min^{-1}, 1:8. $R^1 = CH_3$, $R^2 = n\text{-}C_4H_9$, (±)-DAIB: data (60, 3.7, 29.6), 0.13 mM min^{-1}, 1.0 mM min^{-1}, 1:8. $R^1 = n\text{-}C_4H_9$, $R^2 = CH_3$, (2*S*)-DAIB: data (20, 30.4, 4.0), 3.2 mM min^{-1}, 0.42 mM min^{-1}, 8:1. $R^1 = n\text{-}C_4H_9$, $R^2 = CH_3$, (±)-DAIB: data (60, 16.9, 2.5), 0.59 mM min^{-1}, 0.088 mM min^{-1}, 7:1. In the reactions using di-*n*-butylzinc benzyl alcohol was obtained in ca. 5% yield.

Saturation-transfer experiment

The dissociation rate constant of ***S–R*** was determined by a saturation-transfer experiment at 40 °C. The samples were prepared in a glove box filled with argon with a dew point of –95 °C, in order to avoid moisture and air which decompose the organozinc complexes.[8,9] ***S–S*** (3.0 mg, 0.0054 mmol) and ***S–R*** (3.0 mg, 0.0054 mmol) were placed in a dry 5-mm NMR tube with a Teflon needle valve. The sealed NMR tube was taken out of the glove box and equipped, under an argon stream, with a Schlenk adapter connected to a vacuum–argon double-manifold line. Toluene-d_8 (0.6 mL) was introduced to the NMR tube through a cannula under a slightly positive pressure of argon. The needle valve was closed, and the solution was subjected to ^1H NMR measurement at 40 °C using a pulse FT NMR spectrometer, JEOL JNM-A 400 (400-MHz ^1H frequency), equipped with an NM-AVT3 variable-temperature unit. Chemical shifts are reported in ppm (δ) downfield from tetramethylsilane, and the coupling constants (*J*) are expressed in Hz. The methyl proton signal of toluene, a contaminant in toluene-d_8, at δ 2.31 was used as a standard. Two sets of signals corresponding to ***S–S*** and ***S–R*** appeared in a 1:1 ratio. ^{1}H signal set for ***S–S***: δ –0.21 (s, 3, $ZnCH_3$), 0.91 (s, 3, CH_3), 0.98–1.04 (m, 1, CH_2), 1.12–1.18 (m, 1, CH_2), 1.33 (s, 3, CH_3), 1.34 (s, 3, CH_3), 1.58–1.64 (m, 1, CH_2), 1.81–1.87 (m, 1, CH_2), 1.97 (d, 1, *J* = 4.9 Hz, CH), 2.26 (d, 1, *J* = 7.3 Hz, NCH), 2.29 (s, 6, $N(CH_3)_2$), 4.10 (d, 1, *J* = 6.8 Hz, OCH). ^{1}H signal set for ***S–R***: δ –0.31 (s, 3, $ZnCH_3$), 0.93 (s, 3, CH_3), 0.97–1.03 (m, 1, CH_2), 1.20–1.27 (m, 1, CH_2), 1.24 (s, 3, CH_3), 1.39 (s, 3, CH_3), 1.57–1.63 (m, 1, CH_2), 1.78–1.83 (m, 1, CH_2), 1.94 (d, 1, *J* = 4.6 Hz, CH), 2.29 (s, 3, NCH_3), 2.33 (d, 1, *J* = 4.4 Hz, NCH), 2.47 (s, 3, NCH_3), 4.28 (d, 1, *J* = 7.3 Hz, OCH). The longitudinal relaxation time (T_1) of the *Zn*-CH_3 signal at δ –0.31 in ***S–R*** (9.0 mM toluene-d_8 solution) at 40 °C was measured 6 times by an inversion recovery method in which accumulation times, pulse delay, and data points of pulse interval were set to 32, 20 s, and 20, respectively. The representative T_1 value was determined to be 2.5 s by averaging the observed T_1 of 2.78, 2.41, 2.35, 2.40, 2.47, and 2.57 s. A series of saturation-transfer experiments were performed on a 9.0 mM/9.0 mM mixture of ***S–S*** and ***S–R*** in toluene-d_8 at 40 °C by magnetization of the *Zn*-CH_3 signal of ***S–R***, with T_1 = 2.5 s, data acquisition time = 2.0 s, and accumulation times = 64. The intensity of the exchange-coupled resonance in the nonsaturated site, ***S–R***, decreased and reached saturation when the sample was irradiated for more than 30 s. Irradiation time (T_{irr}, s) and % decrease of signal intensity (A) were as follows: (5.0, 8.2), (7.5, 9.5), (10, 10.1), (12, 10.5), (15, 10.8), (20, 11.1), (25, 11.5), (30, 11.7), (35, 11.7), (40, 11.8). Three saturation-transfer experiments for the determination of k_2 were carried out at 40 °C by irradiating the *Zn*-CH_3 protons of ***S–S*** at δ –0.21 for 60 s, and observing the loss of the *Zn*-CH_3 signal intensity at δ –0.31. As the degree of saturation transfer from ***S–S*** to ***S–R*** was halved because of the participation of the *R* unit in ***S–R***, the observed %A values were doubled for calculating M/M_0 ratios which correspond to 100 – 2 x %A. M/M_0 ratios thus determined were 67.2, 70.6, and 71.8. Substitution of the averaged M_{hetero}/M_0 ratio, 69.9, and T_1, 2.5 s, into the Bloch equation the dissociation rate constant was determined to be 1.7×10^{-1} s^{-1}. The measurement of the degree of saturation transfer from the C(2)-H signal of ***S–S*** to that of ***S–R*** at 40 °C gave the k_2 value of 1.9×10^{-1} s^{-1}. In this set of experiments the parameters T_1 and M/M_0 were 1.7 s and 75.4.

ACKNOWLEDGEMENT

This work was aided by Grand-in-Aid for COE Research (No. 07CE2004) from the Ministry of Education, Science, Sports and Culture, Japan.

REFERENCES AND NOTES

1. Kitamura, M.; Suga, S.; Kawai, K.; Noyori, R. *J. Am. Chem. Soc.* **1986**, *108*, 6071–6072. Noyori, R.; Suga, S.; Kawai, K.; Okada, S.; Kitamura, M.; Oguni, N.; Hayashi, M.; Kaneko, T.; Matsuda, Y. *J. Organomet. Chem.* **1990**, *382*, 19–37. For the first report on the amino alcohol promoted asymmetric ethylation of benzaldehyde, see: Oguni, N.; Omi, T. *Tetrahedron Lett.* **1984**, *25*, 2823–2824.
2. Review: Noyori, R.; Kitamura, M. *Angew. Chem. Int. Ed. Engl.* **1991**, *30*, 49–69.

3. Noyori, R.; Suga, S.; Kawai, K.; Okada, S.; Kitamura, M. *Pure Appl. Chem.* **1988**, *60*, 1597–1606.
4. Oguni, N.; Matsuda, Y.; Kaneko, T. *J. Am. Chem. Soc.* **1988**, *110*, 7877–7878.
5. Bolm, C.; Schlingloff, G.; Harms, K. *Chem. Ber.* **1992**, *125*, 1191–1203.
6. Early reports on the nonlinear effect in asymmetric reactions. Sharpless epoxidation of geraniol and oxidation of sulfides: Puchot, C.; Samuel, O.; Duñach, E.; Zhao, S.; Agami, C.; Kagan, H. B. *J. Am. Chem. Soc.* **1986**, *108*, 2353–2357. Hajos-Wiechert intramolecular aldol reaction: Agami, C.; Levisalles, J.; Puchot. C. *J. Chem. Soc., Chem. Commun.* **1985**, 441–442. Agami, C. *Bull. Soc. Chim. Fr.* **1988**, 499–507. Other asymmetric reactions showing nonlinear effect. Oxidation of sulfides: Komatsu, N.; Hashizume, M.; Sugita, T.; Uemura, S. *J. Org. Chem.* **1993**, *58*, 4529–4533. Meerwein-Ponndorf-Verley reduction: Evans, D. A.; Nelson, S. G.; Gagné, M. R.; Muci, A. R. *J. Am. Chem. Soc.* **1993**, *115*, 9800–9801. Reduction of acetophenone by diisopinocamphenyl chloroborate: Girard, C.; Kagan, H. B. *Tetrahedron: Asymmetry* **1997**, *8*, 3851–3854. Ene reaction: Terada, M.; Mikami, K. *J. Chem. Soc., Chem. Commun.* **1994**, 833–834. Diels–Alder reaction: Iwasawa, N.; Hayashi, Y.; Sakurai, H.; Narasaka, K. *Chem. Lett.* **1989**, 1581–1584. Mikami, K.; Motoyama, Y.; Terada, M. *J. Am. Chem. Soc.* **1994**, *116*, 2812–2820. Kobayashi, S.; Ishitani, H.; Araki, M.; Hachiya, I. *Tetrahedron Lett.* **1994**, *35*, 6325–6328. Silylcyanation of benzaldehyde: Hayashi, M.; Matsuda, T.; Oguni, N. *J. Chem. Soc., Chem. Commun.* **1990**, 1364–1365. Conjugate addition of organometallics to α,β-unsaturated carbonyl compounds: Bolm, C.; Ewald, M.; Felder, M. *Chem. Ber.* **1992**, *125*, 1205–1215. Tanaka, K.; Matsui, J.; Suzuki, H. *J. Chem. Soc., Perkin Trans. 1* **1993**, 153–157. Rossiter, B. E.; Eguchi, M.; Miao, G.; Swingle, N. M.; Hernández, A. E.; Vickers, D.; Fluckiger, E.; Patterson, R. G.; Reddy, K. V. *Tetrahedron* **1993**, *49*, 965–986. Zhou, Q.-L.; Pfaltz, A. *Tetrahedron* **1994**, *50*, 4467–4478. de Vries, A. H. M.; Jansen, J. F. G. A.; Feringa, B. L. *Tetrahedron* **1994**, *50*, 4479–4491. Nitro-aldol reaction: Sasai, H.; Suzuki, T.; Itoh, N.; Shibasaki, M. *Tetrahedron Lett.* **1993**, *34*, 851–854. Allylation of aldehydes using organotin compounds: Keck, G. E.; Krishnamurthy, D.; Grier, M. C. *J. Org. Chem.* **1993**, *58*, 6543–6544.
7. The extent of the nonlinearity is highly dependent on the reaction conditions.[8]
8. Kitamura, M.; Okada, S.; Suga, S.; Noyori, R. *J. Am. Chem. Soc.* **1989**, *111*, 4028–4036.
9. Kitamura, M.; Suga, S.; Niwa, M.; Noyori, R. *J. Am. Chem. Soc.* **1995**, *117*, 4832–4842.
10. Kitamura, M.; Suga, S.; Niwa, M.; Noyori, R.; Zhai, Z.-X.; Suga, H. *J. Phys. Chem.* **1994**, *98*, 12776–12781.
11. Yamakawa, M.; Noyori, R. *J. Am. Chem. Soc.* **1995**, *117*, 6327–6335.
12. Evans, D. A. *Science* **1988**, *240*, 420–426.
13. Corey, E. J.; Yuen, P.-W.; Hannon, F. J.; Wierda, D. A. *J. Org. Chem.* **1990**, *55*, 784–786.
14. For the structural origin of the differences of the homochiral and heterochiral dimers, see: Kitamura, M.; Yamakawa, M.; Oka, H.; Suga, S.; Noyori, R. *Chem. Eur. J.* **1996**, *2*, 1173–1181.
15. Guillaneux, D.; Zhao, S.-H.; Samuel, O.; Rainford, D.; Kagan, H. B. *J. Am. Chem. Soc.* **1994**, *116*, 9430–9439. In Kagan's reservoir effect, catalytic species are considered to be preserved as their associates. See also, Blackmond, D. G. *J. Am. Chem. Soc.* **1997**, *119*, 12934–12939.
16. For the nonlinear effect based on catalyst activation, see: Matsukawa, S.; Mikami, K. *Enantiomer* **1996**, *1*, 69–73. Mikami, K.; Matsukawa, S. *Nature* **1997**, *385*, 613–615. Ohkuma, T.; Doucet, H.; Pham, T.; Mikami, K.; Korenaga, T.; Terada, M.; Noyori, R. *J. Am. Chem. Soc.* **1998**, *120*, 1086–1087.
17. The dimer mechanism of Figure 2 should be seriously considered under some special conditions, e.g. at very high concentrations of the catalyst and reactants.
18. Noller, C. R. *Org. Synth. Collective Vol.* **1943**, *2*, 184–187.
19. Mathre, D. J.; Thompson, A. S.; Douglas, A. W.; Hoogsteen, K.; Carroll, J. D.; Corley, E. G.; Grabowski, E. J. J. *J. Org. Chem.* **1993**, *58*, 2880–2888.
20. Brown, H. C.; Cho, B. T.; Park, W. S. *J. Org. Chem.* **1988**, *53*, 1231–1238.